

N76-28276

## SHAPE OPTIMIZATION OF DISC-TYPE FLYWHEELS

By Richard S. Nizza

Lockheed Missiles & Space Company, Inc.

### ABSTRACT

Recent developments in the field of flywheel powered electrical energy storage systems has prompted the need for a better understanding of the varied design and analytical criteria that must be considered in the selection of a flywheel. Techniques have been developed for presenting an analytical and graphical means for selecting an optimum flywheel system design, based on system requirements, geometric constraints and weight limitations. The techniques for creating an analytical solution are formulated from energy and structural principals. The resulting flywheel design relates stress and strain pattern distribution, operating speeds, geometry, and specific energy levels. The design techniques incorporate the lowest stressed flywheel for any particular application and achieve the highest specific energy per unit flywheel weight possible. Stress and strain contour mapping and sectional profile plotting reflect the results of the structural behavior manifested under rotating conditions. This approach toward flywheel design is applicable to any metal flywheel, and permits the selection of the flywheel design to be based solely on the criteria of the system requirements that must be met, those that must be optimized, and those system parameters that may be permitted to vary.

### INTRODUCTION

This paper describes a procedure for designing an optimum flywheel shape based on the constraints of geometry, speed and stress so as to maximize energy density. The design procedure described relies on the application of linear elastic structural mechanics and the laws of conservation of energy and momentum. Little work has been reported in maximizing the energy density of solid disc flywheels. Much work however has gone into the design of turbine blades and discs, and electric generators and motors, which are perhaps the closest entity to the energy storage flywheel. The basic structural laws under which flywheels, turbine blades, generators and motors behave are the same but their functions, based on different design objectives, are different.

The energy density of a flywheel is represented by the simple relationship:

$$E = K_S \frac{\sigma}{\rho} \quad (1)$$

where  $E =$  energy density

$K_S =$  flywheel shape factor (dimensionless)

$\sigma =$  material working stress

$\rho =$  material density

Flywheel shape factors for several geometries are shown in Table 1. For disc flywheels the shape factor can approach 1.00. The disc shaped flywheel that produces this high a shape factor has constant stresses throughout. This is attributed to the fact that each unit volume of material is stressed equally to a predetermined working stress level and therefore produces the largest amount of energy possible. The flywheel shape that produces this constant stress is exponential in profile.

Equation (2) expresses the summation of forces in a flywheel (Reference 2).

$$\frac{d(XY\sigma_r)}{dX} - Y\sigma_t + \frac{\rho}{g} W^2 X^2 Y = 0 \quad (2)$$

For uniform strength the tangential and radial stresses must be equal and of constant value throughout.

Therefore,

$$\sigma_t = \sigma_r = \sigma = \text{constant}$$

Equation (2) can be restated as

$$\frac{d(XY)}{dx} - Y + \frac{\rho}{g\sigma} W^2 X^2 Y = 0 \quad (3)$$

and by integrating,

$$\ln \frac{Y}{Y_o} = - \frac{W^2 X^2 \rho}{2g\sigma} \quad (4)$$

Applying the boundary conditions, at  $X = X_R, Y = Y_R$

$$\frac{\rho W^2}{2g\sigma} = \frac{1}{X_R^2} \ln \frac{Y_o}{Y_R} \quad (5)$$

Substituting Equation (5) into Equation (4),

$$\frac{Y}{Y_o} = e^{-\left(\frac{X}{X_R}\right)^2 \ln \left(\frac{Y_o}{Y_R}\right)} \quad (6)$$

where  $X$  = radius  
 $Y$  = thickness at radius  $X$   
 $Y_o$  = hub thickness  
 $Y_R$  = tip thickness  
 $X_R$  = tip radius

Equation (6) gives the normalized thickness as a function of the normalized radius and the hub-to-tip thickness ratio. This equation represents the profile configuration for the constant stress flywheel geometry. According to Equation (6), the disc, even though with infinitely decreasing thickness, is prolonged to infinity. But practically, the disc is limited by a cylindrical boundary or radius  $X_R$  at which it has a thickness  $Y_R$ . Although the theoretical flywheel of infinite diameter would have a shape factor of 1.00, the practical flywheel of finite radius  $X_R$  would have a shape factor less than 1.00. In order to improve the shape factor of this exponentially shaped finite diameter flywheel, the author has chosen to take some of the material that theoretically existed between the finite diameter and infinity and place it near the rim of the flywheel producing a constant thickness section running from a point on the surface to the rim. The utilization of a flat tip as the means for improving the flywheel shape factor, in lieu of an exponentially flaired tip, was chosen for two reasons: number one, the shape factor difference between a flaired and a flat tip was found to be insignificant, and secondly, the manufacturing and machining operations are considerably simplified by having a flat tip rather than a flaired tip. The question of how much constant thickness material should be added to the flywheel must now be determined. Since it is the objective to improve the shape factor as much as possible, it is necessary to solve Equation (1) in terms of the shape factor,  $K_S$ , for the various stresses and energy densities associated with each flatted tip flywheel that is generated for each hub-to-tip thickness ratio used in Equation (6). An analytical evaluation must first be performed to evaluate the resulting stresses and energy densities for each flywheel geometry.

One such analytical method developed at Lockheed Missiles & Space Company utilizes a computer program based on two dimensional stresses and strains developed in rotating machinery. These relationships were then expanded (Reference 3) and culminated in the computer program. A typical set of results are shown in Table 2. Tangential stresses, radial stresses and flywheel thicknesses are presented for various radii starting at the rim and extending to the hub. Once the stresses are determined the program then utilizes Equation (1) to calculate the shape factor from the calculated kinetic energy and maximum flywheel stress. A maximum shape factor is then obtained for each hub-to-tip thickness ratio by iteratively evaluating different flatted tips that begin at different percent radii.

Figure 1 represents the results of the relationship between the flywheel shape factor and the hub-to-tip ratio. The point at which the optimum

flat begins has an optimum value which varies with the hub-to-tip thickness ratio. By applying the appropriate flat tip as the means for optimizing the flywheel shape factor for a particular hub-to-tip ratio, it can be recognized that for hub-to-tip ratios less than 1.00, the appropriate flat tip would extend from the tip to the hub, and the flywheel shape would be that of a flat unpierced disc having a shape factor of 0.606.

### FLYWHEEL PARAMETRIC TRANSFORMATIONS

By increasing the hub-to-tip ratio, the shape factor is improved and becomes 1.00 at a hub-to-tip ratio of infinity. There are instances when a high hub-to-tip ratio may not be practical, such as when geometric constraints limit the axial length of the hub. It is therefore desirable to determine the effects of changing parameters on the rest of the system. A set of parametric relationships for relating flywheel diameters, speeds, weights, kinetic energy levels, operating stresses and thicknesses permits an easy determination of the effects on each parameter when one or two are changed. Equations (7), (8), and (9) express these relationships, and can be used for the flywheel shapes generated by Equation (6) having fixed hub-to-tip ratios.

$$\frac{\sigma_N}{\sigma_o} = \left(\frac{D_N}{D_o}\right)^2 \left(\frac{W_N}{W_o}\right)^2 \quad (7)$$

$$\frac{THK_N}{THK_o} = \left(\frac{W_o}{W_N}\right)^2 \left(\frac{D_o}{D_N}\right)^4 \left(\frac{KE_N}{KE_o}\right) \quad (8)$$

$$\frac{WT_N}{WT_o} = \left(\frac{THK_N}{THK_o}\right) \left(\frac{D_N}{D_o}\right)^2 \quad (9)$$

where  $\sigma$  = working stress  
 $D$  = flywheel diameter  
 $W$  = flywheel speed  
 $KE$  = kinetic energy  
 $THK$  = flywheel thickness  
 $WT$  = flywheel weight

A specific example is used to demonstrate the application of these equations for a flywheel having a kinetic energy of 12 kilowatt-hours. This is shown in Figure 2 for several flywheels from three to four feet in diameter. The stagger of the data points is caused by the quantizing error in selection of either 75 or 80 percent flat value for the optimum hub-to-tip ratio. Since the optimum flat lies between these two values a smooth curve in actuality joins the optimum points.

The curves represent a family of varying diameters for a particular kinetic energy level. It is reasonable to assume that the kinetic energy requirements are already known for a desired application. The requirements for the operating speed, or the maximum flywheel stress will further restrict the number of available flywheel design selections. If we permit the flywheel speed to vary, we can superimpose a family of flywheel speeds on Figure 2 indicative of a specific kinetic energy and operating stress level. This was done for an operating stress level of 100 ksi. By utilizing a series of plots similar to Figure 2, reflecting various operating stress levels, a more complete selection of flywheel geometries is possible. These curves represent a means for selecting an optimum geometry flywheel based on the kinetic energy requirements, volumetric limitations, and desired flywheel life (reflected through operating stress level). Once a selection is made, a stress profile may be performed using the two dimensional stress program of Reference 3, which produces results similar to those of Table 2. If upon examination of the results of this initial computer run, the flywheel selected is found to be satisfactory, a much more rigorous, three dimensional, stress-strain examination can be performed using a finite element computer program. A process of contour mapping of the stresses and strains developed under rotating conditions for each and every point within the flywheel can then be made. Figures 3 through 6 show contours for radial, tangential, axial, and axial shear stresses for a quarter section view of a 12 kilowatt-hour flywheel. Figures 7 and 8 show the radial, tangential, axial and axial shear stress distribution along an axis of symmetry, perpendicular to the axis of rotation. The graphs are plotted from right to left. The radial and tangential stresses are maintained at the maximum for almost 80% of the radius and decrease only at the tip.

These techniques permit a very accurate determination of all stresses throughout a homogeneous flywheel, and provide all the quantitative information necessary to perform sensitivity tradeoff studies. This allows a flywheel to be geometrically optimized for a given application in a precise, quick, and economical fashion. The desirability of a constant stress and homogeneous material was assumed; however, in manufacturing thick forgings the metallurgical composition can vary considerably from the core to the surface as well as from the hub to the rim. The effects of the resulting stress pattern variations, developed within the material, must be taken into account and applied to the optimization procedure presented. Such methods have been developed at Lockheed Missiles & Space Company in the form of additional computer programs that evaluate the effects of non-homogeneity of the flywheel material.

## REFERENCES

1. Lawson, L. J. , "Design and Testing of High Energy Density Flywheels for Application to Flywheel/Heat Engine Hybrid Vehicle Drives," Intersociety Energy Conference, P-38, Paper 719150, New York: Society of Automotive Engineers, Inc. , 1971.
2. Stodola, H. , Steam and Gas Turbines, Vol. 1. McGraw-Hill Book Co. , Inc. , New York, 1927.
3. Gilbert, R. R. , et al. , Flywheel Feasibility Study and Demonstration, Final Report to Environmental Protection Agency/Air Pollution Control Office, under contract EHS 70-104, April 30, 1971.

Table 1. Flywheel shape factors for various geometries

Flywheel Geometry	Shape Factor $K_S^*$
Constant-stress disc ( $OD \rightarrow \infty$ )	1.00
Modified constant-stress disc (typical)	0.931
Truncated conical disc	0.806
Flat unpierced disc	0.606
Thin rim ( $ID/OD \rightarrow 1.0$ )	0.500
Shaped bar ( $OD \rightarrow \infty$ )	0.500
Rim with web (typical)	0.400
Single filament (about transverse axis)	0.333
Flat pierced disc	0.305
*From Ref. 1.	

Table 2. Flywheel geometry and stress distribution

FLYWHEEL PARAMETERS

SPEED ----- 1382 RAD/SEC  
 MATERIAL DENSITY ----- .985 LBS/CU-IN  
 POISSONS RATIO ----- .30  
 YOUNG'S MODULUS ----- 30000.0E+03  
 TEMP. EXP. COEFFICIENT ----- 7300.0E-09  
 TOTAL TEMP. DIFFERENCE ----- .0 DEG-F  
 OUTSIDE RADIUS ----- 21.0000 INCHES

FLYWHEEL DESIGN FACTORS

MEAN TANGENTIAL STRESS ----- 108721 PSI  
 MOMENT OF INERTIA ----- 400.453 LB-IN-SEC<sup>2</sup>  
 KINETIC ENERGY ----- 382417805 IN-LBS  
 12.0022 KWH  
 WEIGHT ----- 1069.41 LB  
 ENERGY DENSITY ----- 359954.08 IN-LBS/LB  
 11.3 WH/LB  
 SHAPE FACTOR ----- .9280  
 RADIAL GROWTH ----- .463714E-01 INCHES

RADIUS (IN)	THICKNESS (IN)	TEMPERATURE (DEG-F)	TANGENTIAL STRESS (PSI)	RADIAL STRESS (PSI)
21.0000	1.2658	.0	66242	0
20.5000	1.2458	.0	72139	13118
20.0000	1.2658	.0	77789	26025
19.5000	1.2458	.0	83184	38729
19.0000	1.2458	.0	88314	51240
18.5000	1.2658	.0	93168	63569
18.0000	1.2658	.0	97734	75727
17.5000	1.2658	.0	101999	87725
17.0000	1.2658	.0	105946	99589
16.5000	1.3466	.0	107729	104940
16.0000	1.4914	.0	104023	105571
15.5000	1.6467	.0	108285	106128
15.0000	1.8124	.0	108519	106621
14.5000	1.9885	.0	108729	107058
14.0000	2.1748	.0	108917	107446
13.5000	2.3712	.0	109086	107791
13.0000	2.5772	.0	109238	108099
12.5000	2.7923	.0	109375	108373
12.0000	3.0158	.0	109499	108619
11.5000	3.2471	.0	109610	108838
11.0000	3.4850	.0	109711	109035
10.5000	3.7287	.0	109802	109211
10.0000	3.9769	.0	109885	109369
9.5000	4.2283	.0	109959	109511
9.0000	4.4815	.0	110027	109639
8.5000	4.7350	.0	110088	109753
8.0000	4.9870	.0	110144	109856
7.5000	5.2360	.0	110194	109948
7.0000	5.4809	.0	110239	110031
6.5000	5.7178	.0	110279	110104
6.0000	5.9470	.0	110316	110170
5.5000	6.1659	.0	110348	110229
5.0000	6.3728	.0	110377	110281
4.5000	6.5660	.0	110403	110326
4.0000	6.7438	.0	110425	110366
3.5000	6.9047	.0	110444	110400
3.0000	7.0472	.0	110461	110429
2.5000	7.1701	.0	110474	110454
2.0000	7.2722	.0	110484	110474
1.5000	7.3527	.0	110491	110490
1.0000	7.4107	.0	110493	110505
.5000	7.4457	.0	110465	110543
.0000	7.4574	.0		

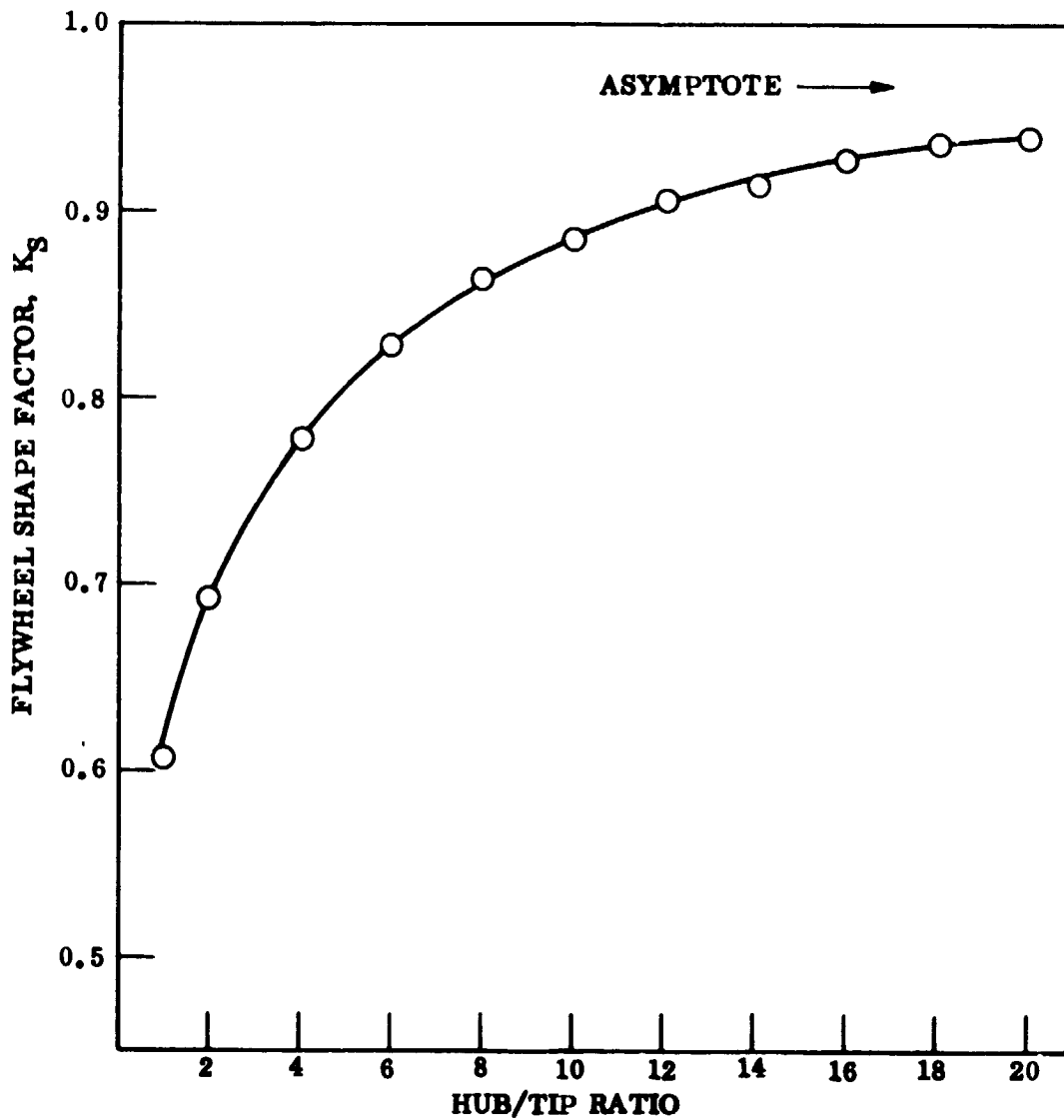


Fig. 1. Flywheel shape factor vs. flywheel hub/tip thickness ratio

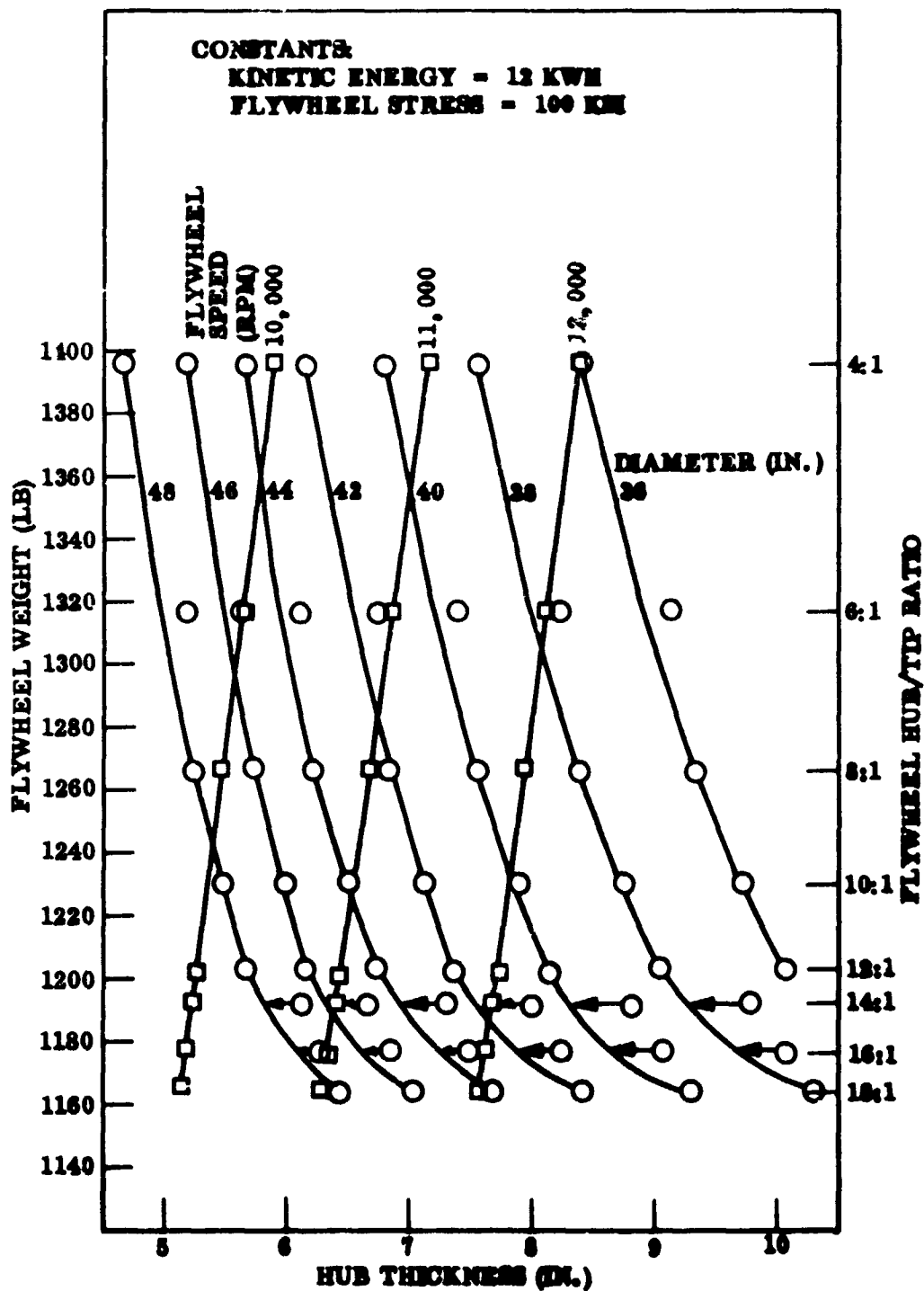


Fig. 2. Flywheel weight and hub/tip ratio vs. hub thickness for several flywheel diameters

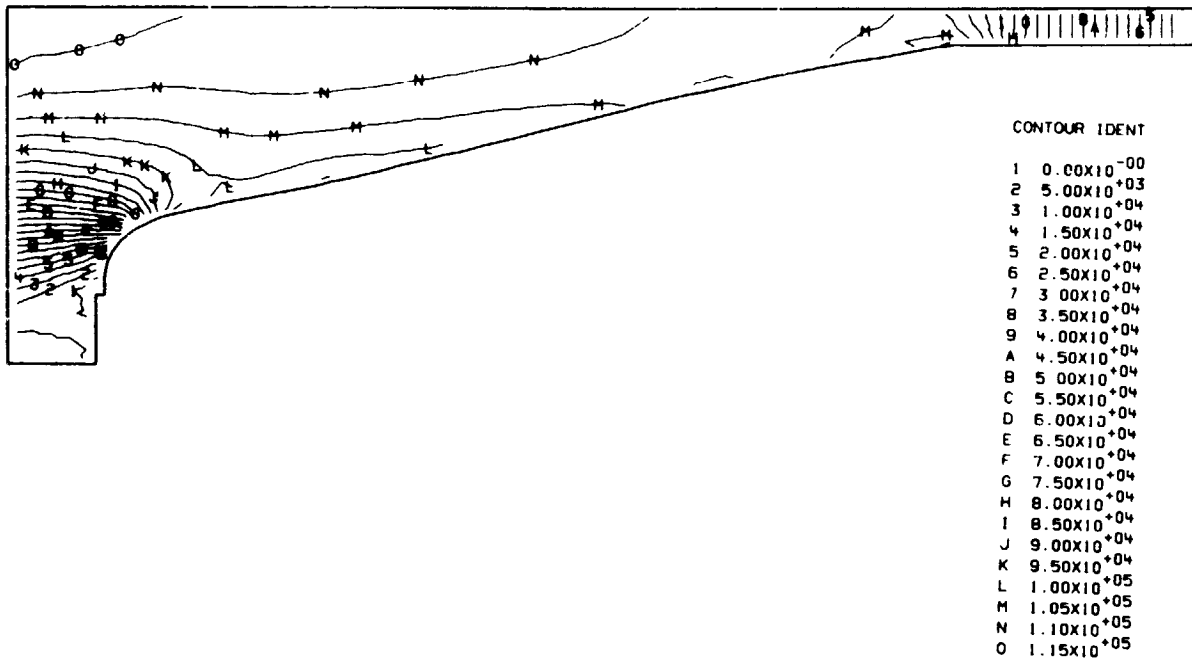


Fig. 3. Contour map of R-stress

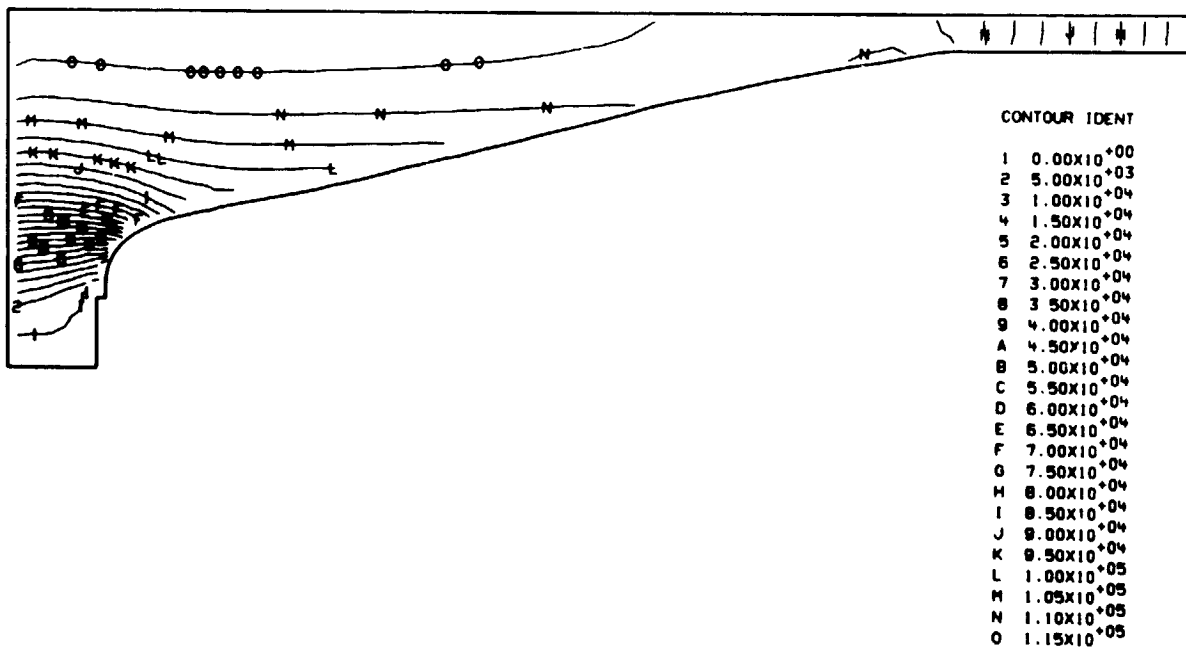


Fig. 4. Contour map of T-stress

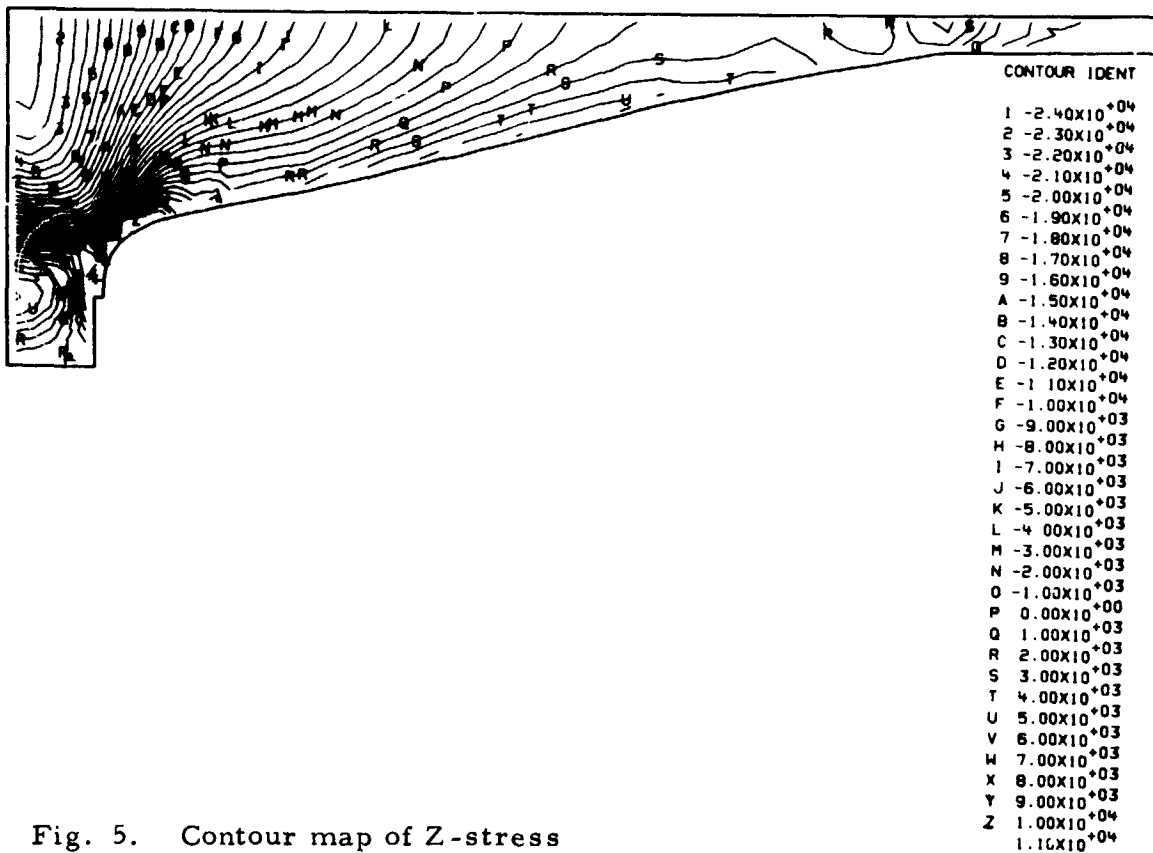


Fig. 5. Contour map of Z-stress

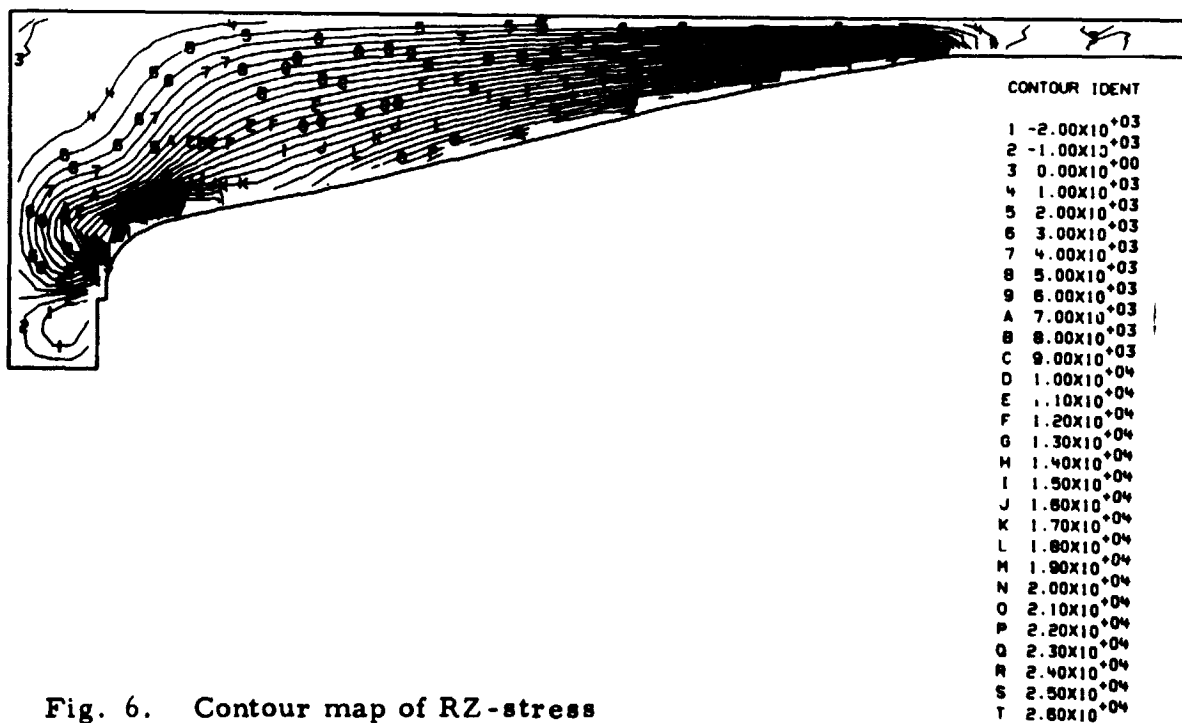


Fig. 6. Contour map of RZ-stress

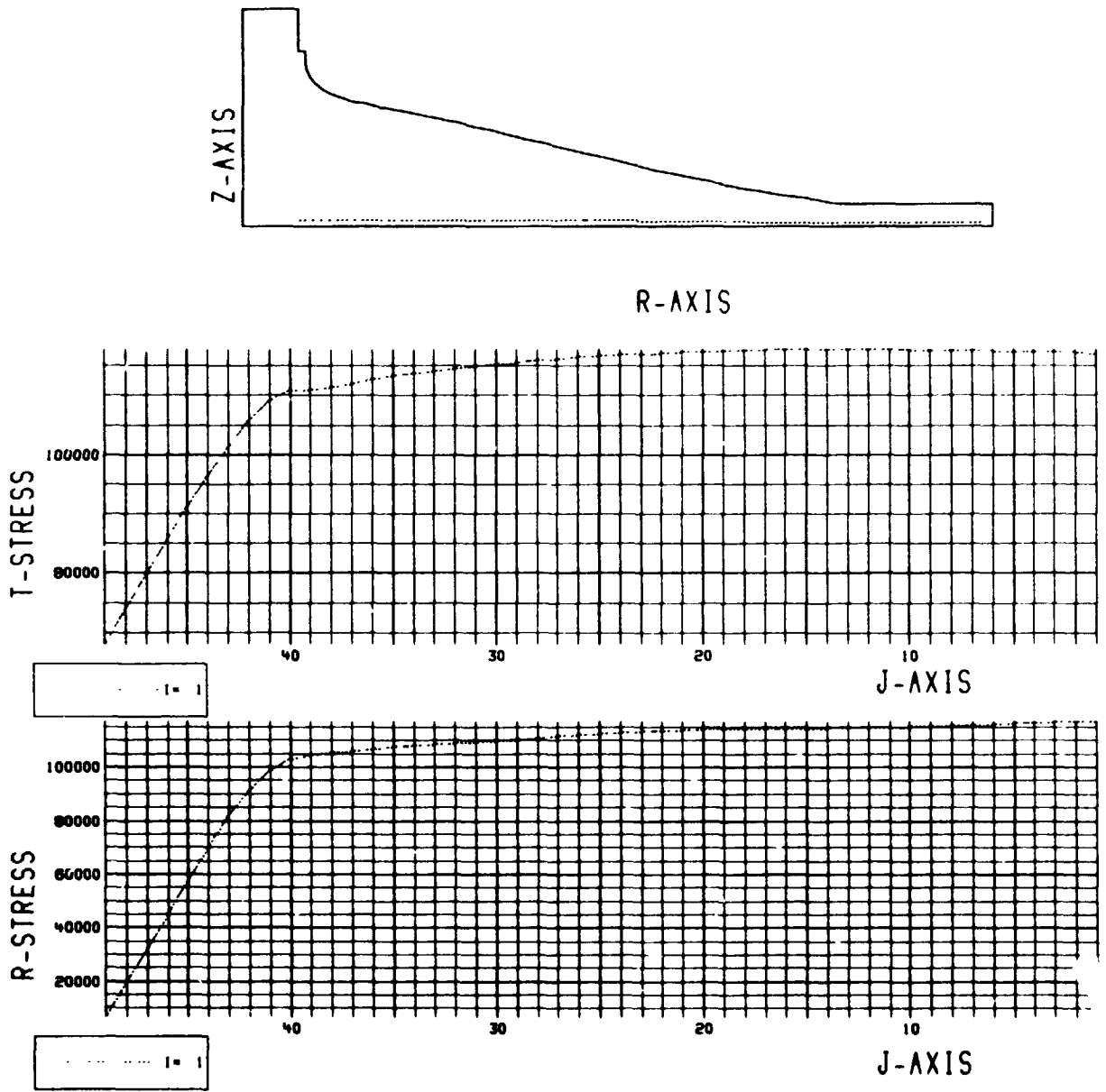


Fig. 7. Radial and tangential stress distribution

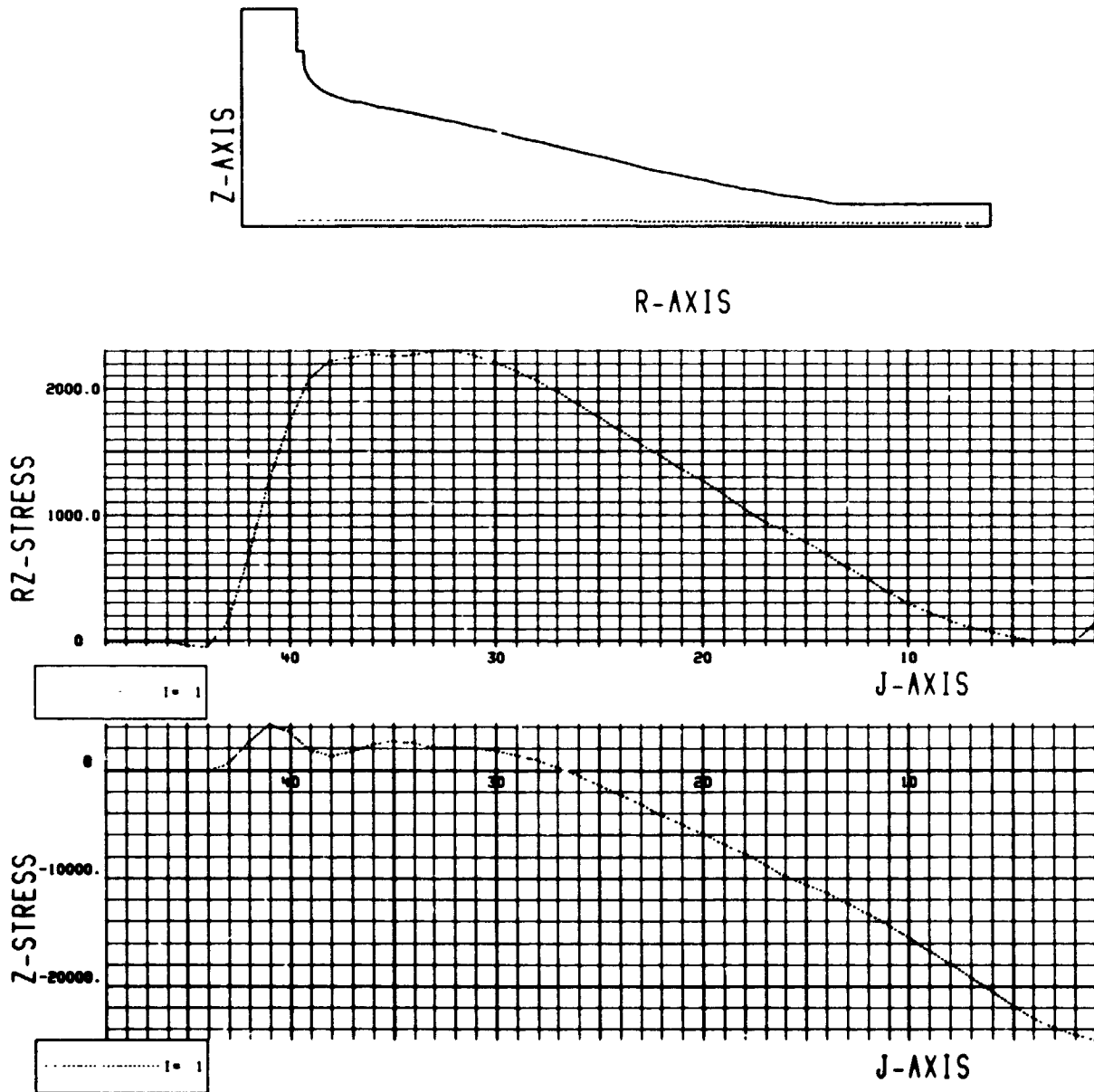


Fig. 8. Axial stress and axial shear stress distribution